Biomechanical design and long-term stability of trees: Morphological and wood traits involved in the balance between weight increase and the gravitropic reaction

T. Alméras, M. Fournier

www.elsevier.com/locate/yjtbi

Biomechanical design and long-term stability of trees: Morphological and wood traits involved in the balance between weight increase and the gravitropic reaction

T. Alméras, M. Fournier

PII: S0022-5193(08)00538-9
DOI: doi:10.1016/j.jtbi.2008.10.011
Reference: YJTBI5332

To appear in: *Journal of Theoretical Biology*

Received date: 20 April 2008
Revised date: 4 September 2008
Accepted date: 9 October 2008

Cite this article as: T. Alméras and M. Fournier, Biomechanical design and long-term stability of trees: Morphological and wood traits involved in the balance between weight increase and the gravitropic reaction, *Journal of Theoretical Biology* (2008), doi:10.1016/j.jtbi.2008.10.011

Biomechanical design and long-term stability of trees: morphological and wood traits involved in the balance between weight increase and the gravitropic reaction.

Alméras T.[a,1,*], Fournier M.[a,2]

[a] INRA, UMR Ecologie des Forêts de Guyane, BP 709, 97310 Kourou, France

[*] Corresponding author : Tancrède Alméras E-mail : t_almeras@hotmail.com
Tel. +334 6714 3431 Fax +334 6714 4792

[1] Present address : LMGC, Université Montpellier 2, Place E. Bataillon, cc 048, 34095 Montpellier cedex 5, France
[2] Present address : Agro Paris Tech, UMR Laboratoire d'Etude de la Ressource Forêt Bois, 14 rue Girardet, 54000 Nancy, France

Abstract

Studies on tree biomechanical design usually focus on stem stiffness, resistance to breakage or uprooting, and elastic stability. Here we consider another biomechanical constraint related to the interaction between growth and gravity. Because stems are slender structures and are never perfectly symmetric, the increase in tree mass always causes bending movements. Given the current mechanical design of trees, integration of these movements over time would ultimately lead to a weeping habit unless some gravitropic correction occurs. This correction is achieved by asymmetric internal forces induced during the maturation of new wood.

The long-term stability of a growing stem therefore depends on how the gravitropic correction that is generated by diameter growth balances the disturbance due to increasing self weight. General mechanical formulations based on beam theory are proposed to model these phenomena. The rates of disturbance and correction associated with a growth increment are deduced and expressed as a function of elementary traits of stem morphology, cross-section anatomy and wood properties. Evaluation of these traits using previously published data shows that the balance between the correction and the disturbance strongly depends on the efficiency of the gravitropic correction, which depends on the asymmetry of wood maturation strain, eccentric growth, and gradients in wood stiffness. By combining disturbance and correction rates, the gravitropic performance indicates the dynamics of stem bending during growth. It depends on stem biomechanical traits and dimensions. By analyzing dimensional effects, we show that the necessity for gravitropic correction might constrain stem allometric growth in the long-term. This constraint is compared to the requirement for elastic stability, showing that gravitropic performance limits the increase in height of tilted stem and branches. The performance of this function may thus limit the slenderness and lean of stems, and therefore the ability of the tree to capture light in a heterogeneous environment.

Key-words

mechanical design, gravitropism, bending stresses, allometry, reaction wood

1. Introduction

Plant stems are slender mechanical structures; their erect habit is mainly constrained by bending movements in response to wind and gravity. Quantitative mechanical design analysis of these bending movements and forces usually focuses on instantaneous mechanical disturbance and safety, using stiffness, breakage or buckling analyses (McMahon and Kronauer, 1976; West et al., 1989; Niklas, 1994a; Niklas 1994b; King et al., 2006; Rowe et al., 2006; Jaouen et al., 2007).

However, gravitropism is a widely studied physiological process (Salisbury, 1993), which plays a key mechanical role in explaining how plant stems can maintain an erect habit, by generating internal forces that counteract the above-mentioned external disturbance by wind or gravity. The control of aerial organ orientation with respect to gravity is necessary to allow the self-standing habit of terrestrial plants, especially in extremely slender, long-lived gigantic structures such as trees (Moulia et al., 2006).

Two different "motors" enable such internal bending forces and resulting axis curvatures: hydrostatic pressure and differential growth in primary tissues, and wood maturation in lignified axes. During the cellular maturation process, at the end of the differentiation of new layers of wood from cambial activity, pre-stresses, which are similar to thermal stresses in engineering materials and are named 'growth stresses' or 'maturation stresses', are generated for the following reasons: i) peripheral wood has a tendency to shrink along the wood grain during secondary wall formation in fibers and ii) as it is glued to a central core of pre-existing wood, it cannot shrink, so it is stretched and put into tension stress (Archer, 1986; Fournier et al., 2006). Asymmetric maturation stresses are usually observed around the stem circumference and cause the axis to bend during growth, because the more stretched side pulls the opposite side. The upper side of leaning stems is usually more stretched than the opposite side, so that the bending movement induced by internal forces counteracts the effect of gravity. This is the basic mechanism of the gravitropic reaction in trees (Wilson and Archer, 1977). As the production of asymmetric strains and stresses is associated with the differentiation of a wood with particular anatomical and chemical features called "reaction wood", this phenomenon has been widely described by wood anatomists (Scurfield, 1973).

Reaction wood is a basal lignophyte growth response and not a derived feature of recent seed plants nor a peculiarity of a few taxonomic entities. It has been described in the most ancestral trees (Scheckler, 2002). Indeed, without this control process, the increasing mass of growing trees would make the stem bend more and more, and gravity would be a terrific ecological constraint: with the currently observed mechanical designs (slenderness ratio, mass distributions and wood stiffness), trees would adopt a weeping habit because of the interaction between growth and gravity (Fournier et al., 1994a; Fournier et al., 2006). Thus, long-term mechanical safety is not only a question of stiffness, breakage or buckling, but also involves a balance

between the slow and long-term mechanical disturbance due to self weight, and the gravitropic correction process related to reaction wood production.

However, due to the lack of practical tools to quantify these processes, their natural variability and their ecological relevance, ecological studies dealing with plant mechanical design have basically focused on the above-mentioned instantaneous mechanical constraints and traits (Poorter et al., 2006; Sterck et al., 2006; Jaouen et al., 2007; Swenson and Enquist, 2007), with no reference to major biomechanical processes studied by physiologists such as tropisms or thigmomorphogenesis (Jaffe, 1980; Moulia et al., 2006). A simple model of gravitropic bending movements has been published, but is restricted to a circular cross-section and concentric growth (Fournier et al., 1994a). When applying this model to an ecophysiological analysis of gravitropic movements of young poplars (Coutand et al., 2007), we noticed that this version is too limited to properly describe some real world situations. More elaborate versions of this model based on finite element methods have been used in growth simulations of entire trees (Fourcaud et al., 2003; Fourcaud and Lac, 2003; Ancelin et al., 2004). These numerical models are suitable for simulation purposes, but cannot be used as a routine tool for analyzing data from large-scale population studies.

In this context, the aim of this paper was to develop a general biomechanical model relating the bending movements (*i.e.* changes in curvature) of woody stems to a finite number of measurable traits describing the stem dimensions, growth allocation and wood properties. Wood properties are density, stiffness and maturation strains and their distribution within the section. Diameter growth defines the increase in cross-section inertia, possibly eccentric, while weight and height growth define the bending loads. We derived simple formulas from the general model that are relevant to large-scale studies. Finally, as mentioned in Fournier et al. (2006), it is of great importance in biomechanical ecological studies to compare the constraint (how the increase in self weight disturbs the orientation), to the correcting process (how wood maturation restores the orientation). The question is similar in ecophysiology when comparing the stimuli (the lean or bending strains induced by gravity and perceived at local or integrated levels) and the responses (strains and curvatures induced by reaction wood formation) (Coutand et al., 2007). Therefore, we compared a model of the disturbance induced by gravity to a model of the correcting gravitropic process. An example is given of how these parameters can be practically estimated. A sensitivity study was performed to quantify the potential effect of morphological traits and wood properties on both processes. By analyzing and comparing these models, we infer theoretical predictions about the mechanical design of the tree and the conditions for long-term biomechanical stability.

2. A general model for the biomechanics of growing woody stems

2.1 Modeling the tree stem as a cantilever beam

Tree stems are usually very slender structures and therefore beam theory is an appropriate framework for studying their mechanical behavior. This general model is valid for any cross-sectional shape and stem taper. The configuration of the stem is defined by the position of any point along its central line, from which can be derived the local orientation angles and the field of curvature. The curvature is defined at each point as the change in local orientation of the stem per unit length. The basic assumption of the beam theory is that the stem deforms so that any plane cross-section remains plane after deformation, and this is generally verified in a slender structure. The deformations are then sufficiently described at the level of any cross-section by the strain perpendicular to the section at a reference point in the section and, more importantly, the gradients of strains within the section[3]. These gradients are equal to the variations in curvature, and can be integrated along the stem to obtain variations in orientation and displacements at any point.

In this study, we assumed that the anchorage is rigid enough to prevent any change in orientation at the emergence point of the stem so that tree movements are only due to the deformations along the stem. The deformations at the level of a given cross-section depend on the loads applied to it by the part of the tree located on the side of the free end, hereafter referred to as the distal part.

2.2 External loads and deformations due to self weight

Loads are described at the level of a section by the resulting force acting perpendicular to the section N_Z and the bending moments B_X and B_Y around the axes of the section's plane (Figure 1). Let O_S be the center of the cross-section at a given position along the stem, expressed in a global reference system (X_T,Y_T,Z_T) associated with the base of the tree, where Z_T is the vertical direction and X_T and Y_T are two cardinal directions. Local axes of the section are defined by Euler's angles θ_S and ϕ_S (see Figure 1). Let $O_SG_S=(x_G,y_G,z_G)$ be the vector joining the center of the section to the center of mass of the distal tree part, expressed in the global reference system. The loads applied on the section by the weight $\vec{W}_S$ of the distal part are given as:

$$\begin{aligned} N_Z^{weight} &= -W_S \cdot \cos\phi_S \\ B_X^{weight} &= W_S \cdot \cos\phi_S \cdot \left(x_G \cdot \sin\theta_S - y_G \cdot \cos\theta_S\right) \\ B_Y^{weight} &= W_S \cdot \left(x_G \cdot \cos\theta_S + y_G \cdot \sin\theta_S\right) \end{aligned} \quad (1)$$

[3] For simplicity, no degrees of freedom in torsion or shear are considered here. Although stem shear and torsion may have important consequences on the mechanical behavior *e.g.* in response to wind, they are considered to be second order effects regarding the self-weight and the gravitropic reaction.

Deformations of the stem in response to gravity generally involve small local strains in the wood, so that it behaves elastically (*i.e.* the strain is reversible) and linearly (*i.e.* the stress in the material is proportional to the strain). The modulus of elasticity (MOE) of wood, E, defines its stiffness, *i.e.* the amount of stress σ generated by a given strain ε:

$$\sigma = E \cdot \varepsilon \tag{2}$$

Here we only consider strains perpendicular to the section, so that the MOE implicitly refers to the MOE measured in the direction of the stem axis. This is generally equal to the modulus of elasticity parallel to the wood grain (but may be different in the case of spiral grain). More generally, wood is a visco-elastic material (*i.e.* it has time-dependent behavior), but the elastic approximation is acceptable if the MOE is measured at the proper time-scale (Alméras et al., 2002). From the basic assumption of the beam theory, the strain perpendicular to section ε is given at any point (x,y) within a section as:

$$\varepsilon(x,y) = \varepsilon_Z + y \cdot C_X - x \cdot C_Y \tag{3}$$

where ε_Z is the axial strain at the reference point, and C_X and C_Y are the curvatures around the X_S and Y_S axes.

The internal loads due to the elastic stress generated within the section are computed as:

$$\begin{aligned} N_Z^{elas} &= \iint_S \sigma(x,y) \cdot dx \cdot dy \\ B_X^{elas} &= \iint_S y \cdot \sigma(x,y) \cdot dx \cdot dy \\ B_Y^{elas} &= -\iint_S x \cdot \sigma(x,y) \cdot dx \cdot dy \end{aligned} \tag{4}$$

Combining equations (2, 3) and (4), the elastic load in response to a deformation (ε_Z, C_X, C_Y) is:

$$\begin{aligned} N_Z^{elas} &= \varepsilon_Z \cdot K_{00} + C_X \cdot K_{01} - C_Y \cdot K_{10} \\ B_X^{elas} &= \varepsilon_Z \cdot K_{01} + C_X \cdot K_{02} - C_Y \cdot K_{11} \\ B_Y^{elas} &= -\varepsilon_Z \cdot K_{10} - C_X \cdot K_{11} + C_Y \cdot K_{20} \end{aligned} \tag{5}$$

The structural stiffness terms $K_{ij} = \iint_S x^i \cdot y^j \cdot E(x,y) \cdot dx \cdot dy$ (where indices i and j here express the power of x and y in the integral) depend on the shape and the size of the section, and on the distribution of the modulus of elasticity.

The static equilibrium is achieved if the internal elastic loads balance the external loads, *i.e.*:

$$N_Z^{elas} = N_Z^{weight} \qquad B_X^{elas} = B_X^{weight} \qquad B_Y^{elas} = B_Y^{weight} \tag{6}$$

Using equations (1), (5) and (6), the deformations ($\varepsilon_Z^{weight}, C_X^{weight}, C_Y^{weight}$) at the level of a stem's section in response to weight load ($N_Z^{weight}, B_X^{weight}, B_Y^{weight}$) can be computed.

2.3 Internal loads and deformations due to wood maturation

Wood maturation induces internal inelastic stresses, due to impeded dimensional changes in the wood. The biochemical processes occurring during the maturation of a piece of wood would induce a relative change in length α if it was isolated, but this maturation strain is impeded by the surrounding material, so that some stress results. Note that the sign of the induced strain and the generated stress is opposite (an impeded contraction α<0 generates a tensile stress σ>0). The maturation induces a significant stress increment only in the recently produced wood because the maturation process is already completed in the inner part of the stem. The loads resulting from maturation stress are:

$$N_Z^{matur} = \iint_S \alpha(x,y) \cdot E(x,y) \cdot dx \cdot dy$$

$$B_X^{matur} = \iint_S y \cdot \alpha(x,y) \cdot E(x,y) \cdot dx \cdot dy \qquad (7)$$

$$B_Y^{matur} = -\iint_S x \cdot \alpha(x,y) \cdot E(x,y) \cdot dx \cdot dy$$

The stem deforms elastically in response to these loads, and the static equilibrium is achieved if the internal elastic loads balance the maturation loads, *i.e.*:

$$N_Z^{elas} = N_Z^{matur} \qquad B_X^{elas} = B_X^{matur} \qquad B_Y^{elas} = B_Y^{matur} \qquad (8)$$

Using equations (5), (7) and (8), the deformations at the level of a stem's section ($\varepsilon_Z^{matur}, C_X^{matur}, C_Y^{matur}$) in response to maturation load ($N_Z^{matur}, B_X^{matur}, B_Y^{matur}$) can be computed.

2.4 Effect of weight and maturation loads in a growing stem

One particular feature of tree biomechanics is that self weight and wood maturation modify the mechanical state of the stem during its formation. As a consequence, standard engineering formulae cannot be used directly because the mechanical state resulting from the simultaneous action of growth and loading is not the same as when a structure is first built, and then loaded (Fournier et al., 1994a). A given piece of wood contributes to support only from the time it is created, and does not support the preexisting loads. This results in specific distributions of stress within the stem section (Kubler, 1987; Fournier et al., 1991a; Fournier et al., 1991b; Fourcaud et al., 2003; Ancelin et al., 2004), with important implications for their biomechanical behavior. To properly compute the mechanical state of a growing structure, an incremental approach is necessary. The elementary load increments (dN_Z, dB_X, dB_Y) during an elementary time step *dt* can be computed, and the resulting elementary deformation increments ($d\varepsilon_Z, dC_X, dC_Y$) can be deduced using equation (5), assuming the stiffness terms K_{ij} are constant during the time step.

As both the effect of self weight and the effect of maturation are related to growth, it is convenient to express the deformation increments as a function of secondary growth, *i.e.* during the time of an increment *dS* in section area. Note however that this formulation is not relevant if variations in load occur without secondary growth. For trees, this can happen for example during particular seasonal events (*e.g.* bud-burst, fruit fall or leaf shedding; Alméras et al., 2004), or if one focuses on the effect of visco-elastic relaxation (Alméras et al., 2002) or the timing of wood maturation (Coutand et al., 2007).

During an elementary growth step, the rate of stem deformation results from the superposition of the effect of increasing weight and maturation. These two contributions can be computed independently from equations (1), (5) and (7), and summed:

$$\begin{aligned} d\varepsilon_Z^{total} / dS &= d\varepsilon_Z^{weight} / dS + d\varepsilon_Z^{matur} / dS \\ dC_X^{total} / dS &= dC_X^{weight} / dS + dC_X^{matur} / dS \\ dC_Y^{total} / dS &= dC_Y^{weight} / dS + dC_Y^{matur} / dS \end{aligned} \quad (9)$$

3. Parametric models for analytical studies and practical applications

3.1 Simplifications: circular cross-section and bilateral symmetry

In order to derive practical formulae, we express growth as a function of changes in diameter *dD* rather than the change in cross-section area *dS*, assuming that the cross-section is circular. For a number of cases (cross-section ovalisation, fluted stem or buttresses), this assumption is not adequate, and specific formulations should be derived by keeping the cross-section area as a reference for secondary growth. Conversion between these alternative formulations is easy, for a circular section: $dS / dD = \pi D / 2$.

Computation of the deformations in the general case requires inversion of the linear equation system (5). However, if the reference point of the section O_S is taken at the neutral line, then the stiffness terms K_{01}, K_{10} and K_{11} vanish, so that the problem is much simplified. Stem movements result mainly from changes in curvature, and we will further assume bilateral symmetry of the problem, so that we are concerned only with the change in curvature in the vertical plane (*i.e.* around Y_S). This assumption is generally sufficient to model the effect of weight and the gravitropic reaction, except if trees with complex geometry are considered, or when studying lateral tropisms, *e.g.* due to the interaction between gravitropism and phototropism (Matsuzaki et al., 2006). Assuming the reference point of the section O_S coincides with the neutral line, the rate of change in curvature with growth can be computed as:

$$dC_Y / dD = \left(dB_Y / dD\right) / K_{20} \tag{10}$$

The flexural stiffness K_{20} depends on the section's geometry and the distribution of material properties within it. It can be written: $K_{20} = E \cdot I$ (11)

where $I = \iint_S x^2 \cdot dx \cdot dy$ is the second moment of area of the section relative to *Y* depending only on its geometry, and *E* is the homogenized MOE, which can be deduced from the distribution of the MOE within the section (or directly measured with a bending test). For a circular cross-section, the second moment of area relative to the geometric center is $I = \pi \cdot D^4 / 64$, so that:

$$dC_Y / dD = \left(dB_Y / dD\right) / \left(E \cdot \pi \cdot D^4 / 64\right) \tag{12}$$

Therefore the resolution of the problem for a particular case reduces to the calculation of the bending moment increment dB_Y generated during a diameter increment *dD*. Bending moments are related to different possible sources of asymmetry. The bending moment due to wood maturation is associated with the circumferential asymmetry of cambial activity (eccentric growth, heterogeneous stiffness and maturation strains). The bending moment due to self weight

is associated with an asymmetry in load distribution, in relation to the stem lean or crown eccentricity. Hereafter we present parametric models for these situations.

3.2 Model of gravitropic change in curvature due to wood maturation

Our reference situation is a circular cross-section of diameter D with bilateral symmetry submitted to a growth increment dD. We assume that the neutral line of the inner section is located at its geometric center, and that its homogenized modulus of elasticity is E. As the new growth ring is assumed to be heterogeneous and eccentric (Figure 2), a long-term reaction would imply a shift in neutral line position, but this situation will be discussed later (see section 4.2). We assume that the stem leans in the X_S+ direction, so that the reaction is expected to create a bending moment $dB_Y^{matur}<0$ and a change in curvature $dC_Y^{matur}<0$ (up-righting movement). Figure 2 illustrates the case of an angiosperm in which the left side of the section is the upper side of the leaning stem, where eccentric growth and tension wood production occur. For a gymnosperm, eccentricity and reaction wood would be located on the right side of the section (lower side of the leaning stem).

The distribution of maturation strains within the new growth ring is defined as a cosine function of the circumferential position θ:

$$\alpha(\theta) = \overline{\alpha} + \Delta\alpha / 2 \cdot \cos\theta \tag{13}$$

where $\overline{\alpha} = (\alpha(0) + \alpha(\pi))/2$ is the mean maturation strain and $\Delta\alpha = \alpha(0) - \alpha(\pi)$ is the difference in maturation strain between the lower and the upper side. The maturation strain is strongly positive in compression wood of gymnosperms, strongly negative in tension wood of angiosperms, and slightly negative in normal wood of all species. Therefore, in a stem tilted in the X_S+ direction and reacting counter-wise, we generally have $\Delta\alpha>0$ and $|\Delta\alpha| > |\overline{\alpha}|$.

The distribution of the modulus of elasticity is given by a similar law:

$$E(\theta) = \overline{E} + \Delta E / 2 \cdot \cos\theta \tag{14}$$

where $\overline{E} = (E(0) + E(\pi))/2$ is the mean MOE and $\Delta E = E(0) - E(\pi)$ is the difference in MOE between reaction wood and opposite wood. As E is strictly positive, its relative variations can always be described by a parameter $k_E = \Delta E/(2\overline{E})$ strictly contained between -1 and 1, and generally much lower than 1 in magnitude. Tension wood is generally stiffer than normal wood (Alméras et al., 2005), and compression wood is generally less stiff (Timell, 1986), so that generally $\Delta E<0$ and $k_E<0$. The distribution of the MOE can thus be written:

$$E(\theta) = \overline{E} \cdot (1 + k_E \cdot \cos\theta) \tag{15}$$

Notice that as $\alpha(\theta)$ and $E(\theta)$ are periodic functions of θ, and as bilateral symmetry has been assumed, the cosine models (13) and (14) remain very general, if they are the first terms of a Fourier analysis of the exact variation $\alpha(\theta)$ and $E(\theta)$. Taking into account the higher order

cosine terms (cos($n\theta$), n>1) of the Fourier analysis does not change the moment calculated in equation (17). For practical reasons, the functions $\alpha(\theta)$ and $E(\theta)$ are usually experimentally characterized from a few (2 to 8) measurements (Fournier and Chanson, 1992; Alméras et al., 2005).

The eccentricity of the growth ring is characterized by a parameter $k_O = dX_O/dR$, where dX_O is the change in position of center of the section relative to a fixed reference (*e.g.* the pith) and $dR = \left(dR(0) + dR(\pi)\right)/2$ is the mean change in radius.

Thus, k_O can also be expressed as $k_O = \left(dR(0) - dR(\pi)\right)/\left(dR(0) + dR(\pi)\right)$, and is contained between −1 and 1, being generally negative for an angiosperm (eccentricity on the left side on Figure 2) and positive for a gymnosperm (eccentricity on the right side on Figure 2).

The thickness of the ring at any circumferential position can be closely approximated by:

$$dR(\theta) = dR \cdot \left(1 + k_O \cos\theta\right) \tag{16}$$

The bending moment around Y generated by the maturation of a growth increment can be computed from equation (7). The maturation strains are zero on the whole section except the outermost wood layer of infinitesimal thickness dR, and thus the bending moment can be computed as a simple integral with respect to θ:

$$dB_Y^{matur} = -dR \cdot \int_0^{2\pi} R \cdot \cos(\theta) \cdot \alpha(\theta) \cdot E(\theta) \cdot \left(1 + k_O \cdot \cos(\theta)\right) \cdot R \cdot d\theta \tag{17}$$

Substituting equations (13, 15) into (17), and integrating with respect to θ we obtain:

$$dB_Y^{matur} = -\pi/2 \cdot \overline{E} \cdot R^2 \cdot dR \cdot \left(\Delta\alpha \cdot \left(1 + 3/4 \cdot k_E \cdot k_O\right) + 2\overline{\alpha} \cdot \left(k_E + k_O\right)\right) \tag{18}$$

Introducing equation (18) into (12), the rate of gravitropic correction, defined as the change in curvature induced by the maturation of an elementary diameter increment can be finally expressed as:

$$\boxed{\frac{dC_Y^{matur}}{dD} = -4 \cdot \frac{e_r}{D^2}} \tag{19}$$

where $1/D^2$ is a dimensional parameter expressing the effect of the size of the section and e_r is a dimensionless parameter expressing the efficiency of the maturation process:

$$e_r = \Delta\alpha \cdot f \cdot \overline{E}/E \tag{20}$$

where $\Delta\alpha$ is the difference in maturation strain between the lower and the upper side and $\overline{E}/E$ is the ratio between the mean MOE of the new ring and the homogenized MOE of the inner section. The effect of circumferential variations in ring width and stiffness is accounted for through a factor f defined as:

$$f = 1 + 3/4 \cdot k_E \cdot k_O + \left(k_E + k_O\right) \cdot 2\overline{\alpha}/\Delta\alpha \tag{21}$$

This factor does not depend on the amount of wood material or its quality, it only depends on their distribution around the circumference, and will be termed “form factor”. The form factor is

1 if the section is homogeneous and concentric, as assumed in previously published models (Fournier et al., 2006).

3.3 Model of bending under self weight at the tree level

We assume a bilateral symmetry of the tree, so that it is sufficiently described in a plane representation (Figure 3) derived from the general case (Figure 1) with θ_S=0 (notice that in this case, torsional forces induced by gravity are rigorously zero). The location of the center of mass G_S of the distal part of the tree depends on the orientation and shape of the stem, and on the possible eccentricity of the crown. The position of G_S relative to the center of the section O_S is defined by its distance h_G and its lean angle ϕ_G, so the total bending moment imposed by the weight is:

$$B_Y^{weight} = W_S \cdot x_G = W_S \cdot h_G \cdot \sin \phi_G \quad (22)$$

The rate of change of the bending moment during diameter growth therefore depends on the rate of change of weight, height and global orientation of the tree. To compute it, explicit information about these parameters and their evolution with diameter is necessary.

Our reference situation is a stem of diameter D_0 at its base and total length H, straight but leaning at an angle ϕ from vertical (here ϕ_S=ϕ_G=ϕ). The stem is assumed to be tapered, and loaded by its own weight and supported masses (branches and leaves). Following other authors (Greenhill, 1881; Niklas, 1994b; Jaouen et al., 2007), we describe the stem taper and the distribution of the total mass M_{tot} by allometric power functions, which generally fit well to experimental data (Jaouen et al., 2007) and are theoretically discussed *e.g.* by Niklas (1994b). For a section located at a distance s from the base, the diameter $D(s)$ and the mass of the distal part $M_>(s)$ are given by:

$$D(s) = D_0 \cdot (1 - s/H)^n \quad (23)$$

$$M_>(s) = M_{tot} \cdot (1 - s/H)^m \quad (24)$$

where n and m are parameters defining the taper and mass distribution, respectively. Parameter n is 0 for a cylindrical stem (no taper) and 1 for a conical stem (linear taper). Parameter m is 1 for a uniformly distributed mass, >1 if the center of mass is closer to the base, and <1 if it is closer to the tip. The volume of the stem V can be deduced from equation (23):

$$V = \frac{\pi}{4} \cdot \frac{H \cdot D_0^2}{(2n+1)} \quad (25)$$

We define the load ratio L of the stem as the ratio between the total mass of the tree M_{tot} and the stem volume V (Jaouen et al., 2007). If the weight of branches, leaves and bark can be ignored, this ratio is equal to the green density of wood. Note however that it significantly differs from the wood basic density (the ratio of oven dry wood mass to fresh volume) usually measured in

biomass studies (King et al., 2006) and sometimes abusively extended to mechanical design studies (Sterck and Bongers, 1998).

Therefore, the weight of the tree above the basal section can be expressed as:

$$W_S = g \cdot V \cdot L = \frac{\pi}{4} g \frac{L}{(2n+1)} H \cdot D_0^2 \tag{26}$$

where g=9.8 $m.s^{-2}$ is the acceleration of gravity.

The location of the center of mass h_G can be computed from equation (24):

$$h_G = H/(m+1) \tag{27}$$

Introducing equations (26) and (27) into (22), the total bending moment at the stem base can be expressed as:

$$B_Y^{weight} = \frac{\pi}{4} g \frac{L \cdot \sin\phi}{(m+1)\cdot(2n+1)} H^2 \cdot D_0^2 \tag{28}$$

To compute the rate of change of the bending moment, we must specify the way each parameter changes with diameter. We will ignore the change in global orientation of the stem during an elementary growth step, and assume that n, m and L are constant during growth, so that we need to know only the relation between height and diameter changes, defined as:

$$b_H = (dH/H)/(dD/D_0) \tag{29}$$

Differentiating equation (28) with respect to D, we obtain:

$$\frac{dB_Y^{weight}}{dD} = \frac{\pi}{2} g \frac{L \cdot \sin\phi \cdot (1+b_H)}{(m+1)\cdot(2n+1)} H^2 \cdot D_0 \tag{30}$$

Using equation (12), the rate of gravitational disturbance, defined as the change in curvature due to the weight associated with an elementary diameter increment, is therefore:

$$\boxed{\frac{dC_Y^{weight}}{dD} = 32 g \frac{L \cdot \sin\phi \cdot (1+b_H)}{E \cdot (m+1)\cdot(2n+1)} \cdot \frac{H^2}{D_0^3}} \tag{31}$$

4. Biomechanical traits and plant scaling in relation to the gravity constraint

The evolution of the shape and orientation of a stem depends on the balance between the effect of weight loads and the gravitropic reaction. We will first illustrate how this information can be obtained empirically, using experimental data from a previous study on plantation trees. Analyzing this real-world situation will show that the correction and disturbance generally closely compensate each other, so that the value of the gravitropic efficiency is a critical parameter determining the biomechanical equilibrium of trees. Then, coming back to the introduced parametric models, we will identify biomechanical traits involved in this equilibrium and study their sensitivity. Finally, we will study how the disturbance and the correction scale with tree size, and deduce a theoretical relation between biomechanical traits, tree allometry and long-term mechanical stability of trees.

4.1 Quantification of weight loads and gravitropic reaction

The model of bending under self weight described earlier is based on a number of assumptions. Some of these assumptions may be inadequate in practical cases, for example if branches are too long to ignore their own lever arm effect, or if the effect of crown eccentricity is studied. A similar analytical model accounting for these parameters could be developed for any specific purpose. Alternatively, a semi-empirical model can be used. If the bending moment is evaluated with an independent method (see below) using a set of trees of different sizes representative of the ontogenetic trend in the population, then the change in bending moment with diameter can be estimated from a statistical regression, and its rate of change obtained by derivation. Using stiffness data, the rate of change in curvature can be deduced.

Practical estimations of the bending moments

To illustrate this method, we used previously published experimental data (Fournier et al., 1990). Nine 30-year-old poplar (*Populus* sp.) trees growing in a plantation in Amance, Meurthe-et-Moselle (France) were felled. Total bending moments applied on the cross-section at breast height were accurately quantified by two independent methods.

The first method was based on direct measurements of strains at the cross-section level as a result of removing the total weight, and then calculation of bending moment using additional measurements of the cross-section dimension and stiffness. Moduli of elasticity were estimated with a 3-point bending-test on 8 samples of sapwood per tree (green wood specimens 20x20x360mm). As the variation between the 8 values was quite low with no systematic variation around the circumference, the mean value was used as a homogenized modulus of elasticity.

The second method used the weight of the trunk (divided into 2.5m long logs), and the crown, as well as geometrical measurements (lean angle of the stem at breast height and radius of the

crown in 8 directions) to estimate the location of the center of mass of the tree and the related bending moment (Fournier et al., 1990). From the comparison of the two methods Fournier et al. (1990) concluded that although inaccurate on twisted trees, the second method was adequate for the 7 vertical or tilted trees. Basic data and bending moments computed with this method are shown in Table 1.

Computation of the rates of disturbance and correction

The bending moment due to the weight and diameter of the tree are statistically related and fit a power function (Figure 4). Assuming that the trend in the population reflects ontogenetic changes in individuals, the rate of change of the bending moment can be taken as the derivative of the relation obtained from regression: $dB_Y^{weight}/dD = 1.37 \cdot 10^7 \cdot D^{3.96}$. The rate of gravitational disturbance can be obtained for each tree using equation (12) and individual diameter and stiffness data.

Maturation strains α along the grain were measured using the two grooves method, *i.e.* strain is provoked by isolating peripheral wood (Fournier et al., 1994b; Yoshida and Okuyama, 2002). Strains were measured with glued strain gauges (Techdis PR10, length 10mm) and an extensometry bridge, at four positions around the circumference for each tree. As expected from mechanical theories of reaction wood and as already observed (Fournier et al., 1994b; Alméras et al., 2005), one side with higher tensile strain values was usually found so that the variation in α could be fitted with the angular variation according to equation (13), allowing the asymmetry of maturation strains $\Delta\alpha$ to be estimated (Table 1). The circumferential variations in the modulus of elasticity were found to be low, and radial variations and eccentricity were not quantified and will be ignored here (their effect will be studied in the next section). Thus the gravitropic efficiency is simply estimated as $e_r = \Delta\alpha$, and the rate of change in curvature due to wood maturation can be estimated from equation (19).

Analyzing the biomechanical equilibrium of a tree population

The computed rates of correction and disturbance (Table 1) show that both rates are variable within the population, and have the same order of magnitude. For trees with a weak reaction (low $\Delta\alpha$), the rate of correction is lower than the rate of disturbance, and thus wood maturation cannot completely compensate for the effect of weight. These trees are predicted to bend more and more if they do not react more intensively. For trees with a marked reaction (high $\Delta\alpha$), the effect of maturation is larger than that of weight, and these trees are probably in an active up-righting process. Overall, the studied sample of trees is close to the biomechanical equilibrium (mean rate of disturbance dC_Y^{weight}/dD = 0.040, SD=0.005, mean rate of correction dC_Y^{matur}/dD = –0.044, SD=0.021). The correction process has the largest variability so that its efficiency, e_r,

appears as a critical parameter to determine individual long-term biomechanical behavior. The next section focuses on the sources of variation of this parameter.

4.2 Quantitative analysis of the gravitropic efficiency

The efficiency of the gravitropic reaction e_r depends at first order on the circumferential distribution of the maturation strain α, and is influenced by other factors such as stiffness gradients and growth eccentricity. In the case of a sinusoidal variation of α, we found that e_r is proportional to the difference $\Delta\alpha$ between the maximal and the minimal maturation strains in the wood ring. Other assumptions about the distribution of α (*e.g.* discontinuous distribution as in Alméras et al. (2004), see appendix) do not qualitatively change the results, but induce an additional correction factor. For example, when half of the ring has maximal α and the other half has minimal α, then the distribution is optimal and the efficiency is 1.27 times that obtained with a sinusoidal variation.

Effects of the asymmetry in wood properties and ring thickness

The effects of stiffness asymmetry and eccentric growth were studied using experimental data from a previous study (Alméras et al., 2005). The mean values of parameters measured in sections of leaning stems of 11 angiosperm and 4 gymnosperm trees from various species are shown in Table 2. The gravitropic efficiency is the product of parameter $\Delta\alpha$ and the form factor f, computed from equation (21). This form factor is shown in Figure 5, for average maturation strain parameters $\overline{\alpha}$ and $\Delta\alpha$, and different levels of k_E and k_O. For angiosperms, the form factor ranges between 1 and 2.22, showing that the within-ring asymmetry in stiffness and thickness can significantly enhance the effect of maturation strains. In the case of gymnosperms the form factor is no more than 1.26, suggesting that the mechanism is in some way less efficient than that used by angiosperms.

Both mechanisms are based on the same basic principle, *i.e.* the asymmetric production of pre-stressed reaction wood: compression wood located on the lower side of the stem for gymnosperms, and tension wood located on the upper side for angiosperms. In both cases, eccentric growth induces a larger ring thickness on the reaction wood side, increasing the efficiency (Figure 5). The mechanisms are basically analogous, since pushing on the lower side and pulling on the upper side have an equivalent effect on the stem. However, there are at least two features for which they are not equivalent. First, stiffness asymmetry k_E increases the efficiency for angiosperms because tension wood is generally stiffer than opposite wood, but decreases it for gymnosperms because compression wood is generally less stiff (Figure 5). Compression wood is therefore intrinsically less efficient because of its lower stiffness. The second difference is related to the action of opposite wood, which is generally in a state of tension for both angiosperms and gymnosperms. For angiosperms, this slight tension on the

lower side partly balances the action of tension wood, and therefore tends to reduce the efficiency. For gymnosperms however, this slight tension on the upper side actively generates the upward bending moment, contributing to the efficiency of the mechanism. When eccentricity occurs, the area of the opposite side is reduced. This reduction has a positive effect for angiosperms, but a negative effect for gymnosperms. This explains why, for comparable levels of $\Delta\alpha$, the effect of k_O on the form factor is lower for gymnosperms than for angiosperms (Figure 5).

In the long term, the circumferential heterogeneity of wood stiffness would induce a shift in the neutral line towards the stiffest side. The position of the neutral line within a heterogeneous section is equal to the ratio K_{10}/K_{00} (see section 2.4 for the definition of these terms). In a section that continuously reacts with asymmetric growth characterized by k_E ad k_O, it can be shown that the position of the neutral line of the section relative to its geometric center is $\left(2\left(k_O+k_E\right)/\left(2+k_Ok_E\right)-k_O\right)\cdot R/3$. The neutral line generally shifts towards tension wood for angiosperms, and towards opposite wood for gymnosperms. This long-term effect tends to decrease the efficiency for angiosperms (because it reduces the lever arm of tension wood) and to increase it for gymnosperms (by increasing the lever arm of compression wood). However, numerical applications of a model exhaustively taking this effect into account show that the shift in neutral line is generally far less than 10% of the radius, and induces only minor changes in the form factor and the gravitropic efficiency.

Effects of the radial variations in stiffness

The effect of radial variations in wood stiffness is contained in the term $\overline{E}/E$ in equation (20), where $\overline{E}$ is the MOE of the outermost wood ring, and E is the homogenized MOE of the whole section. This factor is 1 if the section is homogeneous, but differs in at least two common situations: for small stems in which the pith, which is much less stiff, has an important radial extension, and for trees in which there is an important radial gradient in stiffness.

Lets us assume that the pith extends into a fraction ρ_p of the wood radius, that the wood stiffness is uniformly equal to $\overline{E}$ and that the pith stiffness is equal to $E_{pith}=\gamma_p\cdot\overline{E}$ (with usually γ_p <<1). Using the theory of composite beams, it can be shown that the homogenized flexural MOE is $E=\overline{E}\cdot\left(1-\rho_p^4\right)+E_{pith}\cdot\rho_p^4$, so that the stiffness ratio factor is:

$$\overline{E}/E=1/\left(1+\left(\gamma_p-1\right)\rho_p^4\right) \qquad (35)$$

Assuming a realistic order of magnitude of γ_p=0.01, the correction is plotted on Figure 6. The effect becomes significant if the pith extends into more that 30% of the wood radius, and can become much more important for very young shoots or hollow stems, increasing the efficiency *e.g.* to 3-fold if the pith extends into 90% of the wood radius.

In larger stems, wood stiffness changes progressively with the age of the cambium because a basic characteristic of trees is that juvenile wood is often less stiff (Zobel and Sprague, 1998; Woodcock and Shier, 2002). Let us assume that there is a linear gradient in wood stiffness from the center to the periphery. Let r_E be the ratio between the stiffness of the wood at the tree periphery $\overline{E}(R) = \overline{E}$ and that near the pith $\overline{E}(0) = r_E \cdot \overline{E}$. It can be easily shown that the stiffness ratio is:

$$\overline{E} / E = 5r_E /(1+4r_E) \qquad (36)$$

This effect is plotted in Figure 7. It does not exceed a few percent for reasonable values of r_E.

4.3 Consequences of biomechanical traits on the long-term stability of tilted stems

In the previous section, we showed that traits related to the cross-sectional anatomy of a stem can have a significant influence on the efficiency of its gravitropic process. In this section, we will use these traits, combined with other morphological traits, to determine a condition for the long-term stability of growing stems. This condition will be compared to the requirements for elastic stability (Greenhill, 1881; McMahon and Kronauer, 1976).

Biomechanical traits determining the gravitropic performance

Changes in curvature due to the weight and maturation depend in the first order on the amount of growth dD. In order to demonstrate how biomechanical traits combine independently of the growth rate, we define the gravitropic performance P_g as the ratio between the rate of correction dC_Y^{matur}/dD and the rate of disturbance dC_Y^{weight}/dD. The gravitropic performance indicates the dynamics of bending at the cross-section level: if it is >1 growth creates an upward curving process, if it is <1 growth creates a downward bending, and if it is =1 the stem section is at biomechanical equilibrium, *i.e.* the curvature does not change when the stem grows. At the stem base where an explicit expression of dC_Y^{weight}/dD has been developed (equation 31), P_g is deduced from equations (19) and (31):

$$P_g = \frac{-dC_Y^{matur}}{dC_Y^{weight}} = \frac{1}{8g} \cdot \overline{E} \cdot \Delta\alpha \cdot f \cdot \frac{1}{L} \cdot \frac{1}{\sin\phi} \cdot \frac{(m+1)\cdot(2n+1)}{(1+b_H)} \cdot \frac{D}{H^2} \qquad (37)$$

P_g is larger if the wood produced is stiff (large $\overline{E}$), with large asymmetry of maturation strains ($\Delta\alpha$), a good form factor (large f, achieved by eccentric growth and a consistent asymmetry in wood stiffness), and if the stem has a low load ratio (L), a low tilt angle (ϕ), a low center of mass (large m), a large tapering coefficient (n), a small ratio of relative height growth to relative diameter growth (b_H), a large diameter (D) and a small height (H).

With the definitions of m, n, L, D, H and b_H borrowed from other authors (see section 3.3.), equation (37) is only suitable at the stem base. However, it is easy to adapt to any cross-section

by taking D, H, L and ϕ of a virtual truncated tree. The performance $P_g(s)$ at any level s can therefore be related to the performance P_g at the stem base:

$$P_g(s) = P_g \cdot \frac{\overline{E}(s)}{\overline{E}} \cdot \frac{\Delta\alpha(s)}{\Delta\alpha} \cdot \frac{f(s)}{f} \cdot \frac{\sin\phi}{\sin\phi(s)} \cdot \left(1-\frac{s}{H}\right)^{3n-m} / \left(1-\frac{s}{H}+b_H\right) \qquad (38)$$

Conditions for steady growth of tilted stems

Let us first assume that P_g is uniformly equal to its basal value, given by equation (37). For a tilted stem to remain straight and tilted, it must keep P_g=1 during growth. Usually, this can be achieved just by adjusting the level of gravitropic reaction, *i.e.* the values of $\Delta\alpha$, f and $\overline{E}$. If the tilt angle ϕ is large, it may also be necessary to adjust morphological parameters (L, m, n, b_H). Biomechanical parameters can exhibit adaptive or ontogenetic variations, but are contained within relatively narrow ranges of value linked to the developmental constraints of their species (Jaouen et al., 2007), so that their maximal value can be regarded as constant during growth. On the contrary, stem dimensions (D and H) increase dramatically during growth. Therefore, if a stem has to remain straight and tilted, the term D/H^2 must remain constant, *i.e.* to satisfy an allometry such that H is proportional to $D^{1/2}$ (b_H=1/2). Moreover, if a stem obeys this allometric rule, one can deduce from equation (37) that the maximal angle at which it can lie sustainably depends on the biomechanical parameters, and is given by P_g=1:

$$\sin\phi_{\max} = \frac{\overline{E} \cdot \Delta\alpha \cdot f \cdot (m+1) \cdot (2n+1) \cdot D}{12g \cdot L \cdot H^2} \qquad (39)$$

If the tilt angle becomes larger than ϕ_{max} because of a mechanical accident or an insufficient reaction, then the stem forms an unstable biomechanical configuration (P_g<1). Indeed, to induce an up-righting movement, the stem must produce new wood, but the weight increment associated with this wood would induce an additional downward bending larger than the attempted correction. Moreover, this downward bending would increase ϕ, which would further reduce P_g, condemning the stem to bend more and more. A stem may recover from such a situation by appropriate timing and location of the reaction along the stem. The performance is generally not uniform along the stem, so that the early up-righting of the parts with the highest performance may lower ϕ and therefore also improve P_g in other parts, allowing a global up-righting movement even if the maximal angle has been locally overshot. Tilted stems actually show such complex reaction patterns (Coutand et al., 2007). Equation (38) suggests that $P_g(s)$ is not necessarily uniform along the stem. If variations in $\Delta\alpha$, f, $\overline{E}$ and ϕ are ignored, then a uniform performance is achieved if $(1-s/H)^{3n-m}/(1-s/H+b_H)$ is also uniform. This is equal to $(1-s/H)^{3n-m-1}$ if b_H=0 (no height growth), and close to $(1-s/H)^{3n-m}$ if b_H is large. P_g is uniform if the exponent ($3n-m$ or $3n-m-1$) is zero. If the exponent is <0, then P_g increases along the stem, so that the greatest constraint is at the stem base. Data on taper n and mass

distribution m of saplings from various tree species (Jaouen et al., 2007) show that $3n-m$ is close to zero (ranging between −0.14 and 0.56), so that P_g does not vary much along the stem. More accurate studies of observed functions $\Delta\alpha(s)$, $f(s)$, $\overline{E}(s)$ and $\sin\phi(s)$ would be necessary to precisely understand the relationship between the variations in P_g along the stem and the kinematics of the up-righting movement (Coutand et al., 2007). Nevertheless, the low value of $3n-m$ shows that in the first order, equation (39) and the allometric relation $H \sim D^{1/2}$ are necessary conditions to maintain the stem straight and tilted in the long term.

Biomechanical constraints related to elastic and gravitropic stability

Greenhill (1881) showed that to keep a constant safety factor against the risk of elastic buckling, the allometric growth of a vertical stem should be such that $H \sim D^{2/3}$. The relationship between critical buckling height H_{crit}, stem basal diameter and biomechanical parameters (adapted from Jaouen et al., 2007) is:

$$H_{crit} = \left(\frac{E \cdot (2n+1) \cdot c^2 \cdot (m-4n+2)^2}{64 \cdot g \cdot L} \right)^{1/3} \cdot D^{2/3} \qquad (40)$$

where c is a function of n and m (see Jaouen et al., 2007). The critical buckling height computed from measured biomechanical parameters (Jaouen et al., 2007) is plotted on Figure 8 as a function of stem basal diameter, and compared to the relation deduced from equation (39), for various tilt angles ϕ.

The results show that maximal stem height may be constrained either by its gravitropic performance or by its elastic stability, depending on its diameter and tilt angle. A stem growing at a given angle is limited by elastic stability until a certain diameter, after which gravitropism becomes more limiting. The two constraints theoretically represent mutually exclusive situations: elastic buckling is defined only for a vertical stem, whereas gravitropic control is relevant only for a tilted stem. A real stem is never perfectly vertical, so that bending movements always occur and some gravitropic control is needed. If the stem is close enough to vertical (ϕ is small so that P_g is large), this control can be easily achieved and only elastic stability limits stem allometry. For a larger tilt angle however, the requirements for gravitropic control quickly become more constraining than elastic stability.

The extent to which allometric growth is limited by either of these biomechanical constraints strongly depends on the value of the biomechanical parameters. For example a mean stem (Figure 8-a) of 20 cm is limited by gravitropism if its angle exceeds 15°, and its maximal height is 30 m. For one particular species (Figure 8-b), a stem of the same diameter would be limited by gravitropism at an angle of 10°, with a maximal height of 20 m. This shows that biomechanical parameters determine constraints on dimensions and orientation.

4.4 Conclusions

We have developed an analytical model of the stem curvature variations due to long-term biomechanical actions during growth. The model uses a differential formulation of the beam theory, adapted to growing structures, to calculate the bending moments and curvatures induced by the increase in tree weight (due to growth) and the asymmetric maturation stress (usually associated with reaction wood formation). From general equations, explicit formulas for further ecological or ecophysiological studies are proposed that assume realistic simplifications but take into consideration anisotropic radial growth (pith eccentricity) and gradients of wood stiffness within the cross-section. By applying the model to previously published data we have checked that gravitational and maturation curvatures are of the same order of magnitude in the real word. We found that the gravitational disturbance is indeed a long-term constraint that must be corrected by the gravitropic reaction to ensure steady growth. The model allows the role played by the different components (size described by diameter and height, allometric relations between mass, height and diameter, wood quality and variations within the cross-section) to be studied. The maturation strain asymmetry is clearly the main motor of the reaction, so that the strong assumptions of simple models used in previous studies (Fournier et al., 1994a; Coutand et al., 2007) are justified *a posteriori*. However, other aspects of growth asymmetry (in ring thickness and wood stiffness), contribute significantly to improve the curving process. These interactions are more significant in angiosperms than in conifers, mainly because of the lower stiffness of the compression wood. Thus, a definition of gravitropic performance P_g has been proposed as the ratio of maturation to gravitational curvatures. The larger this indicator, the more effectively can the tree control its angle. P_g is given explicitly as a function of stem morphological parameters and wood biomechanical parameters. At the critical steady limit P_g=1, the tree maintains its angle when it grows. This limit P_g=1 can be associated with a critical lean, expressing the angle above which a stem of given dimensions can no longer remain stable or move closer to vertical, *i.e.* the limit below which the stem can sustainably control its posture (Moulia et al., 2006). By examining the effects of size on this limit, an allometric relation between height and diameter has been proposed, which ensures that at each stage of height growth, diameter growth will be able to maintain the stem below the critical lean. Comparisons between this long-term stability allometry ($H \sim D^{1/2}$) and the elastic stability ($H \sim D^{2/3}$) show that the requirements for gravitropic control can be more constraining than elastic stability for tilted trunks or branches. This theoretical work gives new insights into the functional significance of tree design and wood quality, adding new concepts and operational analytical formulas to the biomechanical ecological toolbox, which up to now has been focused on safety against buckling, wind throw or wind break. In reality, tree stems are never perfectly vertical, and this situation is biomechanically unstable the effect of additional weight must be corrected. Thus the maximum size at which the stem can sustain this tilted situation depends on

the gravitropic performance. We believe that this constraint may be of major biological significance: it limits the ability of stems to move away from verticality, even when lean is a great advantage for maximizing light capture, as is the case for branches, and also for main stems in response to competition with neighbors or heterogeneity of the environment, for instance on slopes (Ishii and Higashi, 1997) or forest edges.

Acknowledgements

This research was carried out as part of the "Woodiversity" project supported by the French National Research Agency (ANR-05-BDIV-012-04). The authors would like to thank Patrick Langbour who provided the poplar data, and Professor Daniel Guitard, now retired, who was at the origin of such discussions in our wood science community 20 years ago.

Cited references

Alméras, T., Costes, E., Salles, J.C., 2004. Identification of biomechanical factors involved in stem shape variability between apricot-tree varieties. Ann. Bot. 93, 1-14.

Alméras, T., Gril, J., Costes, E., 2002. Bending of apricot-tree branches under the weight of axillary productions: confrontation of a mechanical model to experimental data. Trees 16, 5-15.

Alméras, T., Thibaut, A., Gril, J., 2005. Effect of circumferential heterogeneity of wood maturation strain, modulus of elasticity and radial growth on the regulation of stem orientation in trees. Trees 19, 457-467.

Ancelin, P., Fourcaud, T., Lac, P., 2004. Modelling of the biomechanical behaviour of growing trees at the forest stand scale. Part 1: development of an incremental transfer matrix method and application to simplified tree structures. Ann. For. Sci. 61, 263-275.

Archer, R.R., 1986. Growth stresses and strains in trees. Springer Series in Wood Science. Timell, E. Springer-Verlag, Berlin, Heidelberg, New-York, 240 p.

Coutand, C., Fournier, M., Moulia, B., 2007. The gravitropic response of poplar trunks: key roles of prestressed regulation and the kinetics of cambial growth versus wood maturation. Plant Physiol. 114, 1166-1180.

Fourcaud, T., Blaise, F., Lac, P., Castera, P., De Reffye, P., 2003. Numerical modelling of shape regulation and growth stresses in trees II. Implementation in the AMAPpara software and simulation of tree growth. Trees 17, 31-39.

Fourcaud, T., Lac, P., 2003. Numerical modelling of shape regulation and growth stresses in trees I. An incremental static finite element formulation. Trees 17, 23-30.

Fournier, M., Baillères, H., Chanson, B., 1994a. Tree biomechanics: growth, cumulative prestresses, and reorientations. Biomimetics. Plenum Press New York London. Plenum Press, NY. Vol. 2.

Fournier, M., Chanson, B., 1992. Mécanique des structures évolutives et auto-adaptatives, le cas des arbres. Partie 2: modélisation biomécanique de la régulation de l'inclinaison d'un *Pinus pinaster* artificiellement incliné. Architecture, Structure, Mécanique de l'Arbre. 5ème séminaire interne. Paris (France). LMGC, Univ. Montpellier II. pp. 77-91.

Fournier, M., Chanson, B., Guitard, D., Thibaut, B., 1991a. Mechanics of standing trees: modelling a growing structure subjected to continuous and fluctuating loads. 1. Analysis of support stresses. Ann. For. Sci. 48, 513-525.

Fournier, M., Chanson, B., Thibaut, B., Guitard, D., 1991b. Mechanics of standing trees: modelling a growing structure subjected to continuous and fluctuating loads. 2. Three-dimensional analysis of maturation stresses in a standard broadleaved tree. Ann. For. Sci. 48, 527-546.

Fournier, M., Chanson, B., Thibaut, B., Guitard, D., 1994b. Measurement of residual growth strains at the stem surface. Observations of different species. Ann. For. Sci. 51, 249-266.

Fournier, M., Langbour, P., Guitard, D., 1990. Mechanics of standing tree - the evaluation of gravitational forces on a tree trunk from the usual tree measurements. Ann. For. Sci. 47, 565-577.

Fournier, M., Stokes, A., Coutand, C., Fourcaud, T., Moulia, B., 2006. Tree biomechanics and growth strategies in the context of forest functional ecology. In: Ecology and biomechanics. Eds. Herrel, A., Speck, T., Rowe, N.P. Taylor & Francis CRC Press. pp. 1-33.

Greenhill, A.G., 1881. Determination of the greatest height consistent with stability that a vertical pole or mast can be made, and the greatest height to which a tree of given proportions can grow. Proc. Cambridge Philos. Soc. 4, 65-73.

Ishii, R., Higashi, M., 1997. Tree coexistence on a slope: an adaptive significance of trunk inclination. Proc. Royal Soc. London 264, 133-140.

Jaffe, M.J., 1980. Morphogenetic responses of plants to mechanical stimuli or stress. Bioscience 30(4), 239-243.

Jaouen, G., Alméras, T., Coutand, C., Fournier, M., 2007. How to determine sapling buckling risk with only a few measurements. Am. J. Bot. 94(10), 1583-1593.

King, D.A., Davies, S.J., Tan, S., Noor, N.S.M., 2006. The role of wood density and stem support costs in the growth and mortality of tropical trees. J. Ecol. 94, 670-680.

Kübler, H., 1987. Growth stresses in trees and related wood properties. Forestry Abstracts 48, 131-189.

Matsuzaki, J., Masumori, M., Tange, T., 2006. Stem phototropism of trees: a possible significant factor in determining stem inclination on forest slopes. Ann. Bot. 98, 573-581.

McMahon, T.A., Kronauer, R.E., 1976. Tree structures: deducing the principle of mechanical design. J. Theor. Biol. 59, 443-466.

Moulia, B., Coutand, C., Lenne, C., 2006. Posture control and skeletal mechanical acclimation in terrestrial plants: implications for mechanical modeling of plant architecture. Am. J. Bot. 3(10), 1477-1489.

Niklas, K.J., 1994a. The allometry of safety-factors for plant height. Am. J. Bot. 81, 345-351.

Niklas, K.J., 1994b. Plant allometry: The scaling of form and process. University of Chicago Press, Chicago, 395 p.

Poorter, L., Bongers, L., Bongers, F., 2006. Architecture of 54 moist-forest tree species: traits, trade-offs and functional groups. Ecology 87, 1289-1301.

Rowe, N.P., Isnard, S., Gallenmüller, F., Speck, T., 2006. Diversity of mechanical architectures in climbing plants: an ecological perspective. In: Ecology and biomechanics. A mechanical approach to the ecology of animals and plants. Eds. Herrel, A., Speck, T., Rowe, N.P. Taylor and Francis CRC Press.

Salisbury, F.B., 1993. Gravitropism: changing ideas. Hort. Rev. 15, 233-278.

Scheckler, S., 2002. Asymmetric cambial growth and reaction wood of the late Devonian progymnosperm Archeopteris. Botany. Madison, Wisconsin. Pyle Conference Center, University of Wisconsin.

Scurfield, G., 1973. Reaction wood: its structure and function. Science 179:647-655.

Sterck, F.J., Bongers, F., 1998. Ontogenic changes in size, allometry and mechanical design of tropical rainforest trees. Am. J. Bot. 85, 266-272.

Sterck, F.J., Van Gelder, H.A., Poorter, L., 2006. Mechanical branch constraints contribute to life history variations across tree species in a Bolivian rainforest. J. Ecol. 94, 1192-1200.

Swenson, N.G., Enquist, B.J., 2007. Ecological and evolutionary determinants of a key plant functional trait: wood density and its community-wide variations across latitude and elevation. Am. J. Bot. 94, 451-459.

Timell, T., 1986. Compression wood in gymnosperms. Springer-Verlag, 2150 p.

West, P.W., Jackett, D.R., Sykes, S.J., 1989. Stresses in, and the shape of, tree stems in forest monoculture. J. Theor. Biol. 140, 327-343.

Wilson, B.F., Archer, R.R., 1977. Reaction wood: induction and mechanical action. Ann. Rev. Plant Physiol. 28, 23-43.

Woodcock, D.W., Shier, A.D., 2002. Wood specific gravity and its radial variations: the many ways to make a tree. Trees 16, 437–443.

Yoshida, M., Okuyama, T., 2002. Techniques for measuring growth stress. Holzforschung 56, 461-467.

Zobel, B.J., Sprague, J.R., 1998. Juvenile wood in forest trees. Springer Series in Wood Science. E. Timell. Springer Verlag, Berlin, Heidelberg, New York, 300 p.

Appendix: Alternative model at the section's level

The model presented at the section level assumed a continuous sinusoidal variation in the wood properties around the circumference. This model fits more or less empirical observations, but in many cases, the transition between reaction wood and normal wood is rather sharp, so that a discontinuous distribution of wood properties may be more adequate. We developed an alternative formulation that takes into account the effect of within-ring reaction wood distribution. Let us assume that the ring is made of two materials: one located on the upper side of the stem (left side of the section), with an angular extension β, and the other on the lower side of the stem (right side of the section) extending at $2\pi-\beta$ (Figure 9). The properties are assumed to be homogeneous in each sector and equal to α_π, E_π on the upper side, and α_0, E_0 on the lower side.

The bending moment due to the maturation of a new ring is deduced from equation (7):

$$dB_Y^{matur} = -\int_{\pi+\beta/2}^{\pi-\beta/2} x(\theta)\cdot\alpha_0\cdot E_0\cdot dR(\theta)\cdot R\cdot d\theta - \int_{\pi-\beta/2}^{\pi+\beta/2} x(\theta)\cdot\alpha_\pi\cdot E_\pi\cdot dR(\theta)\cdot R\cdot d\theta$$

The change in curvature due to the maturation of the new ring can be put in the same form as equation (19), with a different value of the form factor:

$$f = \frac{4}{\pi}\sin\frac{\beta}{2} + k_O\cdot s_\beta + k_O\cdot k_E + \frac{2\overline{\alpha}}{\Delta\alpha}\cdot\left(\frac{4}{\pi}k_E\cdot\sin\frac{\beta}{2} + k_O + 2k_O\cdot k_E\cdot s_\beta\right)$$

$$\text{with :}\quad s_\beta = 1-(\beta+\sin\beta)/\pi$$

If the reaction wood extends across half of the circumference ($\beta=\pi$), f reduces to:

$$f_{(\beta=\pi)} = \frac{4}{\pi} + k_O\cdot k_E + \left(\frac{4}{\pi}k_E + k_O\right)\cdot\frac{2\overline{\alpha}}{\Delta\alpha}$$

Definition and units of symbols (in order of occurrence)

X_T, Y_T, Z_T	Global reference system associated with the tree [m]
O_S	Center of the cross-section
X_S, Y_S, Z_S	Local reference system associated with the section [m]
ϕ_S, θ_S	Lean and azimuth angle of the normal to the section [rad]
G_S	Center of mass of the part of the tree distal to the section
W_S	Weight of the part of the tree distal to the section [N]
N_Z, B_X, B_Y	Loads: normal force parallel to Z_S and bending moment around X_S and Y_S
ε_Z, C_X, C_Y	Deformations: strain at the center, and changes in curvature around X_S and Y_S
σ	Stress [N.m^{-2}]
ε	Strain
α	Induced maturation strain
A	Cross-section area [m^2]
D	Cross-section diameter [m]
K_{ij}	Structural stiffness terms of the cross-section $K_{ij} = \iint_S x^i \cdot y^j \cdot E(x,y) \cdot dx \cdot dy$
I	Moment of inertia of the cross-section [m^4]
E	Homogenized modulus of elasticity of the section [N.m^{-2}]
θ	Circumferential position in the section [rad]
$\alpha(\theta)$	Maturation strain in the new ring at circumferential position θ
$\overline{\alpha}$	Mean maturation strain in the new ring $\overline{\alpha} = (\alpha(0) + \alpha(\pi))/2$
$\Delta\alpha$	Contrast of maturation strain in the new ring $\Delta\alpha = \alpha(0) - \alpha(\pi)$
$E(\theta)$	Modulus of elasticity in the new ring at circumferential position θ
$\overline{E}$	Mean modulus of elasticity in the new ring $\overline{E} = (E(0) + E(\pi))/2$
ΔE	Difference in modulus of elasticity in the new ring $\Delta E = E(0) - E(\pi)$
k_E	Relative asymmetry of modulus of elasticity $k_E = \Delta E / (2\overline{E})$
k_O	Parameter of eccentricity $k_O = dX_O/dR$
e_r	Efficiency of the gravitropic mechanism $e_r = \Delta\alpha \cdot f \cdot \frac{\overline{E}}{E}$
f	Form factor related to the distribution of material properties within the section
β	Parameter defining the tangential extension of reaction wood [rad]

ρ_p	Ratio of pith radius to wood radius in the section
E_{pith}	Modulus of elasticity of the pith [N.m^{-2}]
γ_p	Ratio between the moduli of elasticity of the pith and wood
r_E	Ratio between the stiffness of the wood at the tree periphery and near the pith
h_G	Distance between the center of the section and the distal center of mass [m]
ϕ_G	Lean angle of the distal center of mass relative to the section [rad]
x_{OG}	Projected horizontal distance between the section and the distal center of mass
D_0	Diameter at the stem base [m]
H	Total length of the stem [m]
ϕ	Lean angle of the stem [rad]
M_{tot}	Total mass of the tree [kg]
$D(s)$	Stem diameter at a distance s from the base [m]
$M_{>}(s)$	Mass of the tree located above a distance s from the stem base [kg]
n	Exponent defining the tapering of the stem
m	Exponent defining the distribution of mass along the stem
V	Stem volume [m^3]
L	Load factor of the stem $L = M_{tot} / V$ [kg.m^{-3}]
g	Acceleration of gravity g=9.8 $m.s^{-2}$.
b_H	Ratio of relative height growth to relative diameter growth $b_H = \frac{dH / H}{dD / D_0}$
P_g	Gravitropic performance

Tables and figure's legends

Figure 1. Schematic representation of a tree submitted to its own weight, and the resulting loads at the level of a given cross-section *S*. O_S is the section's center, $\vec{W}_S$ is the weight of the distal part (*i.e.* the part of the tree located above the section), G_S is the location of the center of mass of the distal part. The local axes (X_S,Y_S,Z_S) of the section are obtained from the global axes (X_T,Y_T,Z_T) by a rotation of θ_S around Z followed by a rotation ϕ_S around Y. At the level of the section, loads result in a normal force N_Z, and bending moments B_X and B_Y (all positive in the figure).

Figure 2. Reference model for a heterogeneous eccentric section of diameter D submitted to a diameter increment dD. The stem is assumed to be leaning in the positive X_S direction, so that the reaction is expected to generate a negative change in bending moment $dB_Y<0$, generating a change in curvature $dC_Y<0$ (*i.e.* up-righting movement). Variations in greyness indicate heterogeneity of the material properties within the new growth ring (see text).

Figure 3. Schematic representation of the effect of self weight in a tree with bilateral symmetry. O_S is the center of a given cross-section, $\vec{W}_S$ is the weight of the distal part, G_S is the location of the center of mass of the distal part, defined by its tilt angle ϕ_G and its distance h_G with respect to O_S. The projected distance between the section and the center of mass is x_G.

Figure 4. Relation between the total bending moment due to self weight (B_Y) and the diameter of trees (D) at breast height. The line is a regression by a power function: $B_Y = 2.76*10^6*D^{4.96}$ (R^2=0.73).

Figure 5. Values of the form factor f for angiosperm and gymnosperm trees obtained from eq. (21) using data from Table 2. The maturation strain parameters $\overline{\alpha}$ and $\Delta\alpha$ are set at the mean values and different levels of the eccentricity parameter k_O and the stiffness asymmetry parameter k_E are compared (white bars: k_E=0, grey bars: k_E=mean value, black bars: k_E=maximal value).

Figure 6. Effect of the pith size on the stiffness ratio ($\overline{E}/E$) influencing the gravitropic efficiency. Parameter ρ_p is the ratio between the radius of the pith and that of the wood.

Figure 7. Effect of a radial gradient in wood stiffness on the stiffness ratio ($\overline{E}/E$) influencing the gravitropic efficiency. Parameter r_E is the ratio between wood stiffness near the periphery and near the core.

Figure 8. Relation between maximal basal diameter and maximal height, for a vertical stem submitted to the risk of elastic buckling (thick red line), and for growing stems leaning at various angles. Data are based on mean gravitropic parameters from Table 2 ($\Delta\alpha$=0.17%, f=1.54) and mechanical and morphological parameters measured in 150 saplings belonging to 15 tropical angiosperm tree species (Jaouen et al., 2007). (a) Using overall mean parameters: E=1.23*10^{10} N.m^{-2}, m=1.62, n=0.66, c=4.72,

L=1340 kg.m^{-3}. (b) Mean stem of a severely constrained species (*Sextonia rubra*): E=8.50*10^{9} N.m^{-2}, m=0.63, n=0.3, c=2.61, L=1438 kg.m^{-3}.

Figure 9. Alternative model of a heterogeneous eccentric section of diameter D submitted to a diameter increment dD. The stem is assumed to lean in the positive X_S direction, so that the reaction is expected to generate a negative change in bending moment $dB_Y<0$, generating a change in curvature $dC_Y<0$ (*i.e.* up-righting movement). The new growth ring is assumed to be made of two distinct materials, extending at an angle β (on the left side) and $2\pi-\beta$ (on the right side).

Table 1. Main data used for computing the rate of disturbance and correction of poplar trees at breast height: trunk diameter (D), lean (ϕ_S), crown eccentricity (x_C = horizontal distance between the tree and the center of the crown), total mass above breast height (M_{tot}) and resulting bending moment (B_Y^{weight}), mean modulus of elasticity in the new ring ($\overline{E}$), asymmetry of maturation strains ($\Delta\alpha$), and computed rates of gravitational disturbance (dC_Y^{weight}/dD) and gravitropic correction (dC_Y^{matur}/dD).

Table 2. Mean and maximal values of parameters influencing the gravitropic efficiency (from Alméras et al., 2005): mean maturation strain ($\overline{\alpha}$), maturation strain asymmetry ($\Delta\alpha$), growth eccentricity (k_O) and asymmetry of the modulus of elasticity (k_E).

Table 1.

Tree n°	D (m)	ϕ_S (°)	x_C (m)	M_{tot} (kg)	B_Y^{weight} (N.m)	$\overline{E}$ (MPa)	$\Delta\alpha$	dC_Y^{weight}/dD (m^{-2})	dC_Y^{matur}/dD (m^{-2})
1	0.26	4.6	1.32	558	3470	8125	841	0.036	-0.052
2	0.23	0.6	0.37	428	651	6345	609	0.046	-0.046
3	0.22	4.0	0.91	348	1273	5895	417	0.050	-0.036
4	0.24	2.0	0.16	467	300	7470	918	0.039	-0.064
5	0.26	0.9	0.19	552	434	7720	861	0.038	-0.051
6	0.22	2.3	0.40	336	496	7560	1022	0.039	-0.083
7	0.23	2.9	0.70	361	1002	7360	156	0.040	-0.012
8	0.27	3.7	0.18	693	604	7580	515	0.039	-0.029
9	0.26	1.7	0.31	622	951	8715	410	0.034	-0.024

Table 2.

		$\overline{\alpha}$ (%)	$\Delta\alpha$ (%)	k_O	k_E
Angiosperms	Mean	-0.14	0.17	-0.23	-0.09
	Max	-0.18	0.28	-0.45	-0.25
Gymnosperms	Mean	0.05	0.15	0.31	-0.18
	Max	0.07	0.20	0.44	-0.26

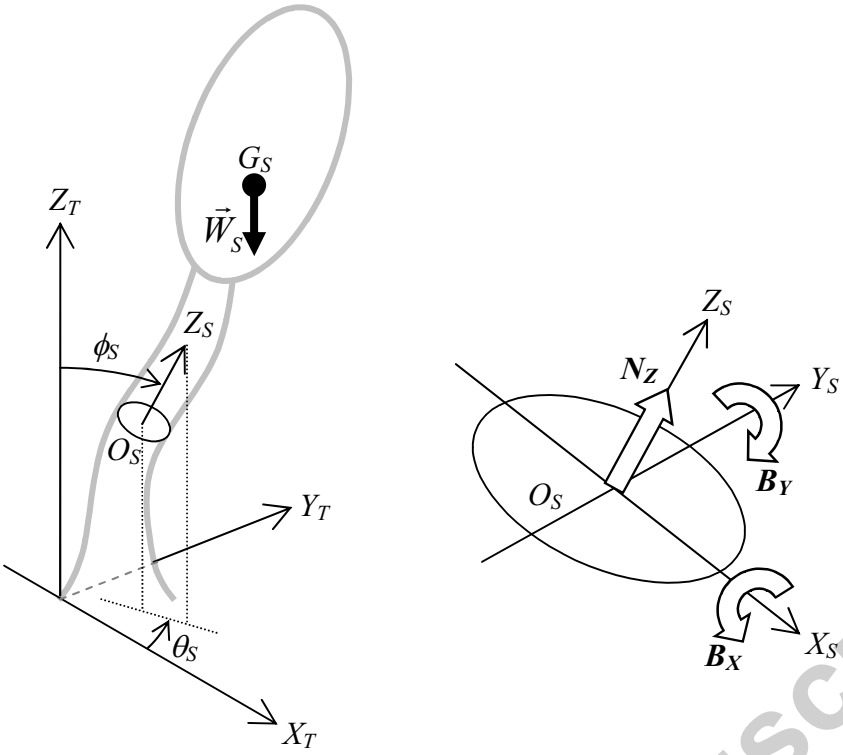

Figure 1.

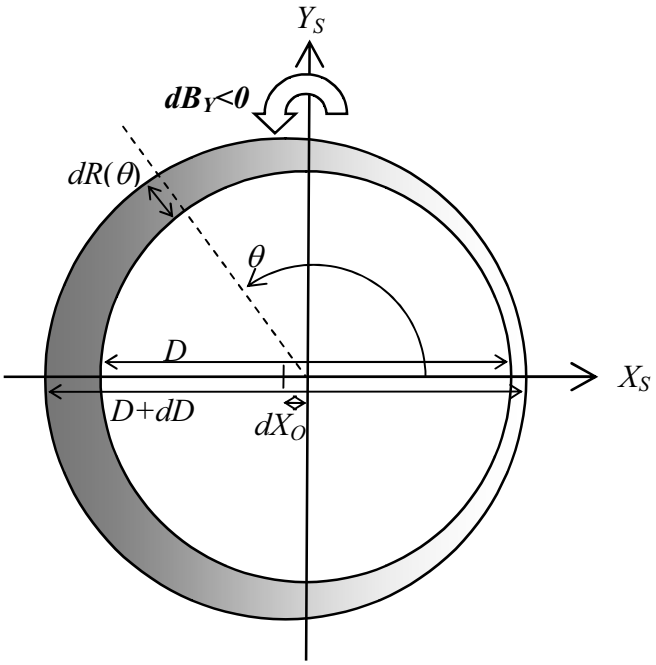

Figure 2.

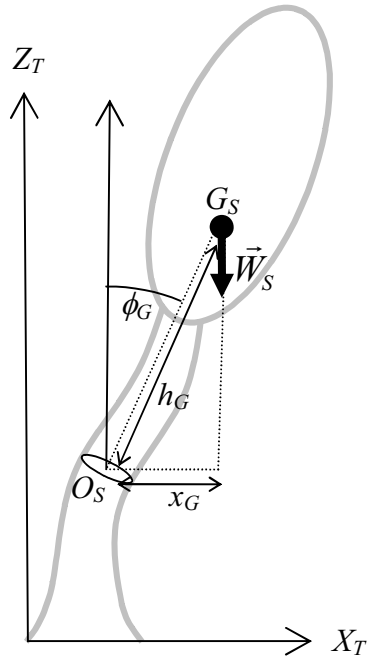

Figure 3.

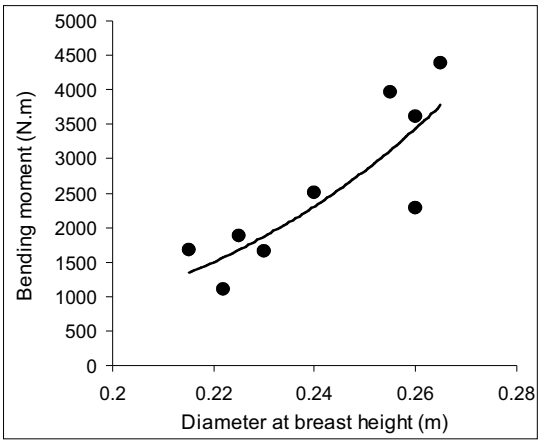

Figure 4.

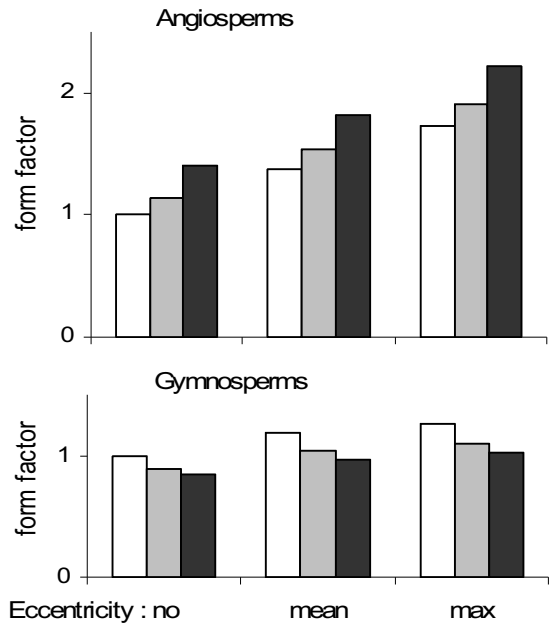

Figure 5.

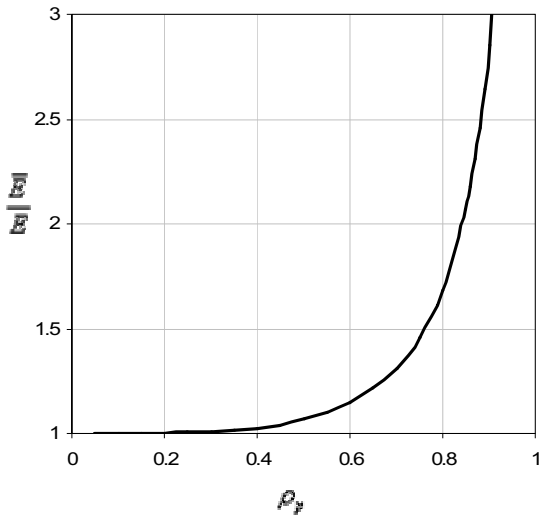

Figure 6.

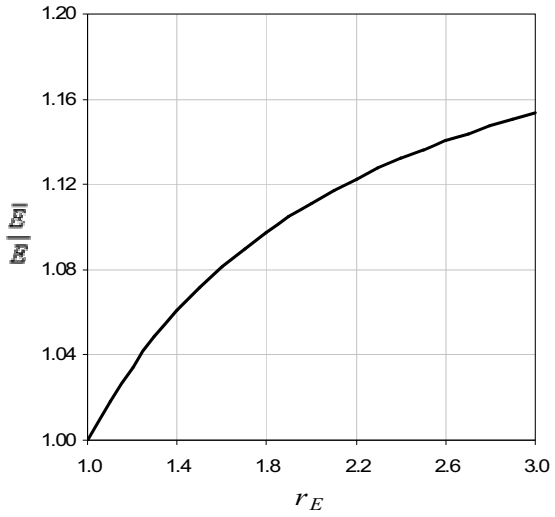

Figure 7.

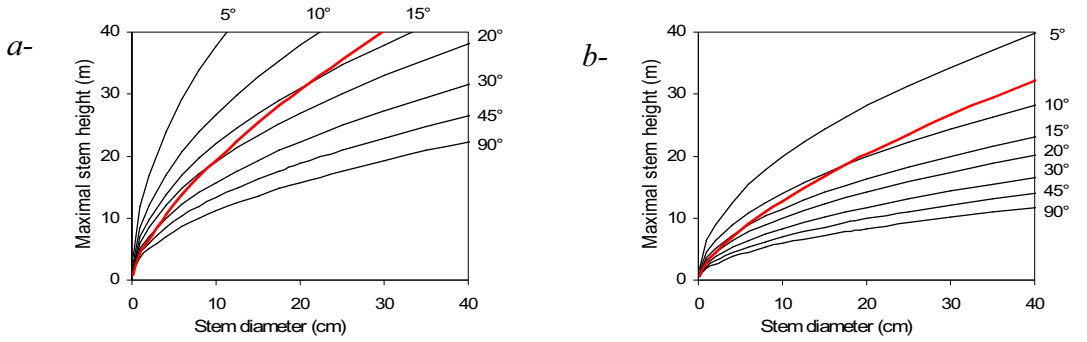

Figure 8.

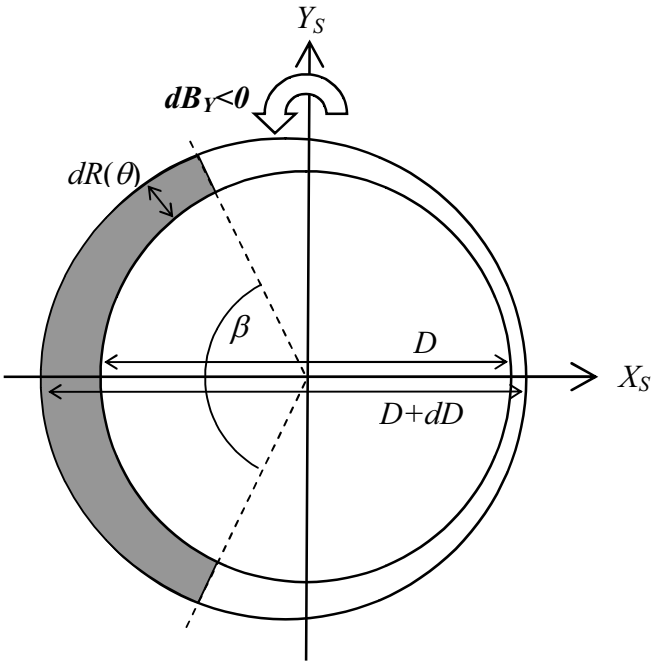

Figure 9.